Article

Infrared Spectroscopy of Gas-Phase Cr Coordination Complexes: Determination of Binding Sites and Electronic States

David T. Moore, Jos Oomens, John R. Eyler, Gert von Helden, Gerard Meijer, and Robert C. Dunbar

J. Am. Chem. Soc., **2005**, 127 (19), 7243-7254• DOI: 10.1021/ja042431d • Publication Date (Web): 22 April 2005

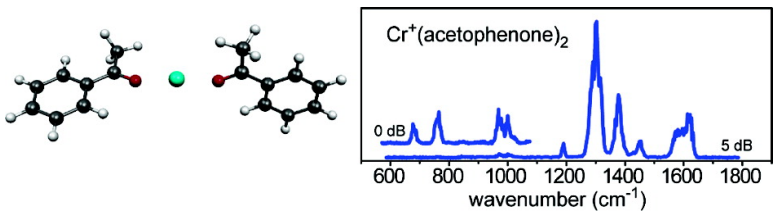

More About This Article

Additional resources and features associated with this article are available within the HTML version:

- Supporting Information
- Links to the 9 articles that cite this article, as of the time of this article download
- Access to high resolution figures
- Links to articles and content related to this article
- Copyright permission to reproduce figures and/or text from this article

View the Full Text HTML

J|A|C|S
ARTICLES
Published on Web 04/22/2005

Infrared Spectroscopy of Gas-Phase Cr^+ Coordination Complexes: Determination of Binding Sites and Electronic States

David T. Moore,[†] Jos Oomens,[†] John R. Eyler,[#] Gert von Helden,[†,§] Gerard Meijer,[†,§] and Robert C. Dunbar*[,‡]

Contribution from the FOM Institute for Plasma Physics "Rijnhuizen", Postbus 1207, 3430 BE Nieuwegein, The Netherlands, Fritz-Haber-Institut der Max-Planck-Gesellschaft, Faradayweg 4-6, 14195 Berlin, Germany, Chemistry Department, University of Florida, Gainesville, Florida 32611-7200, Chemistry Department, Case Western Reserve University, Cleveland, Ohio 44118

Received December 16, 2004; E-mail: robert.dunbar@case.edu

Abstract: Infrared spectra were recorded for a series of gas-phase Cr^+ complexes using infrared multiphoton dissociation (IRMPD) in a Fourier transform ion cyclotron resonance (FT-ICR) mass spectrometer. The functionalized aromatic ligands (acetophenone, anisole, aniline, and dimethyl aniline) offer a choice of either aromatic ring-π or n-donor-base binding sites. Use of the FELIX free electron laser light source allowed convenient, rapid scanning of the chemically informative wavelength range from approximately 500 to 1800 cm^{-1}, which in many cases characterized the preferred site of metal binding, as well as the electronic spin state of the complex. Mono-complex ions, Cr^+(ligand), for anisole, aniline, and dimethyl aniline and bis-complex ions, $Cr^+(ligand)_2$, for anisole, aniline, and acetophenone were produced by ligand attachment to laser-desorbed Cr^+ ions in the FT-ICR cell. The photodissociation yields plotted as a function of wavelength were interpreted as approximations to the infrared absorption spectra and were compared with computed spectra of different possible geometries and spin states. Clear-cut diagnostic features in the spectra of the acetophenone, anisole, and aniline complexes showed the sites of Cr^+ attachment to be the carbonyl oxygen site for acetophenone (bis-complex) and the ring-π site for anisole and aniline (both mono- and bis-complexes). The bis-complexes of aniline and anisole are low-spin (probably doublet) states, while the mono-complexes of these same ligands are high-spin (sextet) states. The dimethyl aniline complex gave a cluttered spectrum in poor agreement with calculations, which may reflect a mixture of binding-site isomers in this case.

Introduction

Complexes of transition metal ions with aromatic molecules are of interest as model systems for understanding many different fundamental phenomena, such as metal−ligand interactions and metal ion solvation.[1−7] Understanding these processes in turn may shed light on more applied topics, such as binding of transition metals in biological systems, which is important across a broad range of processes, for example, photosynthesis and electron transport,[8,9] oxygen binding and transport,[10] metal chelation,[11] activity of antibiotic[12] and anti-Alzheimers[13] agents, pathological redox chemistry,[14] and the synthesis of DNA binding agents.[15] In virtually all of these cases, the binding of the transition metal occurs through one or more functionalized aromatic moieties, with the specific site being either an electronegative atom (e.g., N or O) or the aromatic ring, as in the well-known cation−π complexes,[6] and thus, the competition between these two types of binding is of fundamental importance.[16] In addition, most of the above processes require a particular electronic (or oxidation) state for the transition metal. This paper focuses on the elucidation by infrared spectroscopy of both of these issues, binding site competition and electronic state determination, for a series of organometallic complexes in the gas phase.

[†] FOM Institute for Plasma Physics "Rijnhuizen".
[§] Fritz-Haber-Institut der Max-Planck-Gesellschaft.
[#] University of Florida.
[‡] Case Western Reserve University.

(1) Eller, K.; Schwarz, H. *Chem. Rev.* **1991**, *91*, 1121.
(2) Diefenbach, M.; Schwarz, H. In *Electronic Encyclopedia of Computational Chemistry*; Schleyer, P. v. R., Schreiner, P. R., Schaefer, H. F., Jorgensen, W. L., Thiel, W., Glen, R. C., Eds.; John Wiley & Sons: Chichester, U.K., 2004.
(3) Leary, J. A.; Armentrout, P. B. *Int. J. Mass Spectrom.* **2001**, *204*, 1.
(4) Freiser, B. S. *Organometallic Ion Chemistry*; Kluwer: Dordrecht, The Netherlands, 1996.
(5) Russell, D. H. *Gas Phase Inorganic Chemistry*; Plenum: New York, 1989.
(6) Ma, J. C.; Dougherty, D. A. *Chem. Rev.* **1997**, *97*, 1303.
(7) Muetterties, E. L.; Bleeke, J. R.; Wucherer, E. J. *Chem. Rev.* **1982**, *82*, 499.
(8) Pierloot, K.; de Kerpel, J. O. A.; Ryde, U.; Olsson, M. H. M.; Roos, B. O. *J. Am. Chem. Soc.* **1998**, *120*, 13156.
(9) Blomberg, M. R. A.; Siegbahn, P. E. M.; Babcock, G. T. *J. Am. Chem. Soc.* **1998**, *120*, 8812.
(10) Collman, J. P.; Fu, L. *Acc. Chem. Res.* **1999**, *32*, 455.
(11) Hu, P.; Sorensen, C.; Gross, M. L. *J. Am. Soc. Mass Spectrom.* **1995**, *6*, 1079.
(12) Ming, L.-J.; Epperson, J. D. *J. Inorg. Biochem.* **2002**, *91*, 46.
(13) Gnjec, A.; Fonte, J. A.; Atwood, C.; Martins, R. N. *Front. Biosci.* **2002**, *7*, d1016.
(14) Hippeli, S.; Elstner, E. F. *FEBS Lett.* **1999**, *443*, 1.
(15) Metcalfe, C.; Thomas, J. A. *Chem. Soc. Rev.* **2003**, *32*, 215.
(16) Ryzhov, V.; Dunbar, R. C. *J. Am. Chem. Soc.* **1999**, *121*, 2259.

A wide range of mass spectrometric approaches have been applied to determine the properties of ionic complexes in the gas phase. In particular, binding reactions and thermochemistry of metal−ion complexes with aromatic organic ligands have been examined using a variety of such approaches, for example, threshold collision-induced dissociation (CID),[17−19] collision-activated dissociation,[11,20,21] radiative association kinetics,[16,22,23] blackbody infrared radiative dissociation (BIRD),[24] threshold photodissociation,[25] time-resolved photodissociation kinetics,[25,26] and ion−molecule reactivity.[27,28] While such mass spectrometric approaches provide detailed information about absolute and relative binding energies and reactivities, they offer only indirect probes of the geometric and electronic structures of the complexes. For structural information, it is almost indispensable to employ a spectroscopic approach. Electronic spectroscopy of gas-phase ions in the visible/ultraviolet wavelength region has been used with success in structural studies of gas-phase ions,[29] but vibrational spectroscopy in the infrared (IR) region is the technique best suited for obtaining structural information on gas-phase ions.

Infrared spectroscopy has long been employed as a tool in condensed phases to study the structure and bonding of transition metal complexes; however, analogous gas-phase results have been difficult to obtain until recently. The advent of intense, tunable infrared sources, such as pulsed optical parametric oscillators (OPOs) in the near-IR[30] and free electron lasers (FELs) in the mid-to-far IR,[31,32] has provided new opportunities for obtaining gas-phase infrared spectra of ions. Results for several ionic transition metal complexes have already been reported,[33−36] and studies in the area have recently been reviewed.[30] A recent and exciting development in this new field is that the vibrational spectra, in addition to providing structural information, can also be used in combination with theoretical predictions to determine the electronic state of the metal centers in gas-phase organometallic complexes.[34,35,37,38]

It is a challenging problem to obtain sufficiently high densities of mass-selected gas-phase ions for carrying out direct IR absorption spectroscopy. The strategy of "action spectroscopy" gives an easier way to obtain similar information about the optical absorption spectrum. Action spectroscopy techniques are based on observation of a secondary change in the system, typically fragmentation, which can be measured with greater sensitivity than the actual changes in the intensity of the incident light. For systems where the binding energy is greater than that of a single IR photon, such as the metal ion−molecule complexes studied here, infrared multiple photon dissociation (IRMPD) can be used to fragment the parent ions; it is then the resulting change in mass of the ions that forms the basis for the action spectroscopy in this case. The principle of resonant photofragmentation via IRMPD has been discussed in detail elsewhere[31,39] and can be summarized as follows. The energy resulting from the absorption of a photon by a molecule or ion is rapidly relaxed to the other vibrational modes via intramolecular vibrational redistribution (IVR). This redistribution does not appreciably shift the original optical transition, and so it remains resonant with the laser, allowing absorption of another photon. In this way, many photons can be rapidly absorbed in a noncoherent fashion, resonantly "heating" the molecule above its fragmentation threshold. This process requires rather high photon fluxes, which is why intense sources such as pulsed OPOs and FELs are needed for such experiments.

Interfacing an FEL to a capable mass spectrometer can enhance the capabilities of an IRMPD experiment by adding more powerful resources of ion synthesis and manipulation. To this end, a Fourier transform ion cyclotron resonance (FT-ICR) instrument was recently interfaced to the Free Electron Laser for Infrared eXperiments (FELIX) at FOM.[40,41] This provides new capabilities at FELIX parallel to the recently established FT-ICR interface at the CLIO FEL facility at Orsay, which has been used for several experiments involving metal−ion clusters.[35,42,43] An early application of this new combined instrument at FOM was an investigation of the structure of the Cr^+-(aniline) and $Cr^+(aniline)_2$ complexes, which offer a real choice between a π coordination site on the aromatic ring versus an n-donor-base site on the nitrogen atom.[36] In fact, the difference between the two sites is so close that different DFT functionals predicted opposite preferences, with B3LYP and MPW1PW91 indicating N-atom and ring-binding, respectively. The IR spectroscopy experiment showed no such ambiguity, and conclusively demonstrated that both the mono- and bis-complexes preferred to bind at the aromatic ring.[36] The present report expands this earlier study, including both further consideration of the aniline complexes and also the study of Cr^+ complexes with several other ligands presenting a choice of binding sites to the metal ions. We refer to the two types of site as "ring" for binding to the aromatic moiety and "side-chain" for binding to an electronegative atom in a functional group. On the basis of computational estimates, the three ligands, acetophenone, anisole, and aniline, form an interesting set, on

(17) Rodgers, M. T.; Armentrout, P. B. *Mass Spectrom. Rev.* **2000**, *19*, 215.
(18) Rodgers, M. T.; Armentrout, P. B. *J. Am. Chem. Soc.* **2002**, *124*, 2678.
(19) Rannulu, N. S.; Amunugama, R.; Yang, Z.; Rodgers, M. T. *J. Phys. Chem. A* **2004**, *108*, 6385.
(20) Schroeter, K.; Wesendrup, R.; Schwarz, H. *Eur. J. Org. Chem.* **1998**, 565.
(21) Satterfield, M.; Brodbelt, J. S. *Inorg. Chem.* **2001**, *40*, 5393.
(22) Dunbar, R. C. In *Current Topics in Ion Chemistry and Physics*; Ng, C. Y., Baer, T., Powis, I., Eds.; Wiley: New York, 1994.
(23) Dunbar, R. C. *J. Phys. Chem. A* **2002**, *106*, 7328.
(24) Dunbar, R. C. *Mass Spectrom. Rev.* **2004**, *23*, 127.
(25) Dunbar, R. C. In *Chemistry and Physics of Gas Phase Ions*; Armentrout, P. B., Ed.; Elsevier: Oxford, 2003; p 403.
(26) Dunbar, R. C. In *Advances in Gas Phase Ion Chemistry*; Babcock, L. M., Adams, N. G., Eds.; JAI Press: Greenwich, CT, 1996; p 87.
(27) Combariza, M. Y.; Vachet, R. W. *J. Am. Soc. Mass Spectrom.* **2002**, *13*, 813.
(28) Lei, Q. P.; Amster, I. J. *J. Am. Soc. Mass Spectrom.* **1996**, *7*, 722.
(29) Dunbar, R. C. In *Chemistry and Physics of Gas Phase Ions*; Armentrout, P. B., Ed.; Elsevier: Oxford, 2003; p 249.
(30) Duncan, M. A. *Int. Rev. Phys. Chem.* **2003**, *22*, 407.
(31) Oomens, J.; Tielens, A. G. G. M.; Sartakov, B.; von Helden, G.; Meijer, G. *Astrophys. J.* **2003**, *591*, 968.
(32) Oomens, J.; van Roij, A. J. A.; Meijer, G.; von Helden, G. *Astrophys. J.* **2000**, *542*, 404.
(33) Fielicke, A.; von Helden, G.; Meijer, G.; Pedersen, D. B.; Simard, B.; Rayner, D. M. *J. Phys. Chem. B* **2004**, *108*, 14591.
(34) Jaeger, T. D.; van Heijnsbergen, D.; Klippenstein, S. J.; von Helden, G.; Meijer, G.; Duncan, M. A. *J. Am. Chem. Soc.* **2004**, *126*, 10981.
(35) Reinhard, B. M.; Lagutschenkov, A.; Lemaire, J.; Maitre, P.; Boissel, P.; Niedner-Schatteburg, G. *J. Phys. Chem. A* **2004**, *108*, 3350.
(36) Oomens, J.; Moore, D. T.; von Helden, G.; Meijer, G.; Dunbar, R. C. *J. Am. Chem. Soc.* **2004**, *126*, 724.
(37) van Heijnsbergen, D.; von Helden, G.; Meijer, G.; Maitre, P.; Duncan, M. A. *J. Am. Chem. Soc.* **2002**, *124*, 1562.
(38) Jaeger, T. D.; Pillai, E. D.; Duncan, M. A. *J. Phys. Chem. A* **2004**, *108*, 6605.
(39) Bagratashvili, V. N.; Letokhov, V. S.; Makarov, A. A.; Ryabov, E. A. *Multiple Photon Infrared Laser Photophysics and Photochemistry*; Harwood Academic Publishers: Chur, Switzerland, 1985.
(40) Oepts, D.; van der Meer, A. F. G.; van Amersfoort, P. W. *Infrared Phys. Technol.* **1995**, *36*, 297.
(41) Valle, J. et al. *Rev. Sci. Instrum.* **2005**, *76*, 023103.
(42) Kapota, C.; Lemaire, J.; Maitre, P.; Ohanessian, G. *J. Am. Chem. Soc.* **2004**, *126*, 1836.
(43) Lemaire, J. et al. *Phys. Rev. Lett.* **2002**, *89*, 273002.

the basis that the first should illustrate complexes bound at the side-chain (carboxymethyl functional group), the second should illustrate ring-bound complexes, and the third presents a genuine challenge to the spectroscopic approach to elucidate its otherwise unpredictable preferred binding site. *N*,*N*-Dimethyl aniline was added to the study in the expectation of learning more about the Cr^+ binding competition, predicted to be very close, between a side-chain nitrogen site and the aromatic ring site.

Another goal of this study is to determine the extent to which the vibrational spectra can identify the electronic states of the complexes. Computation gives firm predictions of high-spin (sextet) complexes for some of the complexes considered here, but the ring-bound bis-complexes of anisole and aniline are not computationally predictable. These complexes may be expected to have low-spin (doublet) configurations since they are 17-electron complexes,[7] and the condensed phase ESR[44,45] and X-ray crystallographic data for $(C_6H_6)_2Cr^+I^-$ [46] support a doublet configuration. In the gas phase, theory predicts that $(C_6H_6)_2Cr^+$ should be a doublet,[34] and the photoelectron spectroscopy[47,48] and CID[49] results are consistent with this. On the other hand, recent investigations of the gas-phase spectroscopy of $(C_6H_6)V^+$ and $(C_6H_6)_2V^+$ indicate that the experimentally observed electronic states are different from those predicted by DFT calculations.[37,38] Thus, it is interesting to see if vibrational spectroscopy can provide more direct confirmation that the chromium ion is in a low-spin doublet electronic state in the ring-bound bis-complexes with aromatic ligands studied here.

Experimental

The experimental setup, based on the coupling of an FT-ICR mass spectrometer with the beam line of FELIX,[41,50] has been extended with a laser ablation source external to the FT-ICR magnet to generate chromium ions. Briefly, the FT-ICR mass spectrometer is based on a 4.7 T actively shielded superconducting magnet (Cryomagnetics, Inc.) and a laboratory-constructed vacuum system and an open, cylindrical ICR cell, and is controlled by a computer using the MIDAS hardware/software interface.[51] A Cr sputtering target (Goodfellow, 99.98% purity) was placed in the vacuum chamber on the magnetic field axis approximately 1 m from the ICR cell, that is, outside the magnet bore. The fundamental of an Nd:YAG laser, with a typical pulse energy of 20 mJ, was mildly focused onto the metal target. Guided only by the weak external magnetic field, the ablated metal ions drifted into the ICR cell, where they were trapped by increasing the voltage on the trapping plates. Coordination complexes were then formed by admitting the vapor ($5-10 \times 10^{-7}$ Torr peak pressure) from above the organic liquid sample of interest through a pulsed valve. A second pulse of He gas (5×10^{-6} Torr peak pressure) was also added in order to stabilize the formation of the complexes. Samples were used as received from the supplier, except for a freeze−pump−thaw cycle to remove dissolved gases.

The four ligands studied were as follows:

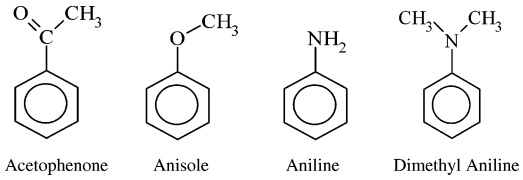

Cr^+ attaches two ligands sequentially for this series of ligands

$$Cr^+ + L \rightarrow Cr^+L \quad (1)$$

$$Cr^+L + L \rightarrow Cr^+L_2 \quad (2)$$

Attachment of a third ligand molecule was not observed in any case. A reaction delay of 2−5 s was used to allow the complex of interest to form and cool via collisions (in the presence of the decaying He pulse) and spontaneous emission to the ambient temperature in the ICR trap, namely, 300 K.[52] Since laser ablation is known to produce significant abundances of metal atoms and ions in excited electronic states,[53] such a delay was considered necessary to ensure that the complexes were in the ground electronic state when the spectra were taken. Following the reaction delay, the parent ion under study (either Cr^+L or Cr^+L_2) was isolated by applying a stored-waveform inverse Fourier transform (SWIFT)[54] pulse to the excite plates of the ICR cell to eject unwanted species. For the bis-complexes, higher peak pressures and longer reaction times were used in order to drive reaction 2 further toward completion. The mass selected complex ions were then irradiated with several (typically 10) pulses from FELIX. For experiments on the mono-complexes, fewer FELIX pulses were generally used than for the bis-complexes. This had the effect of reducing the time that the ions were subjected to irradiation, thus reducing the depletion of mono-complex parent ions by ion molecule reactions (specifically by reaction 2) during this time. Each FELIX pulse (∼5 μs) consists of a 1 GHz train of micropulses (∼10 μJ energy), and the duration of these micropulses (∼1 ps) determines the bandwidth of the radiation, which is typically 0.2−0.5% of the central wavelength. The wavelength is continuously tunable between 3 and 250 μm; in this work, we investigated the range between 500 and 1800 cm^{-1} (20−5.5 μm). Upon resonant absorption of multiple photons, the complex can reach internal energies beyond the dissociation threshold and, hence, undergo fragmentation.

The Cr^+L mono-complexes were observed to dissociate via ligand removal yielding the bare Cr^+ ion

$$Cr^+L \xrightarrow{h\nu} Cr^+ + L \quad (3)$$

The Cr^+L_2 complexes showed loss of one or both ligands

$$Cr^+L_2 \xrightarrow{h\nu} Cr^+L + L \quad (4)$$

$$Cr^+L_2 \xrightarrow{h\nu} Cr^+ + L + L \quad (5)$$

After irradiation with FELIX, a standard FT-ICR excite/detect event[55] was applied, and the time-domain transient was averaged four times for each wavelength point and stored on a PC. The mass spectrum was recovered using an FFT algorithm, and all fragment channels were

(44) Feltham, R. D.; Sogo, P.; Calvin, M. J. *J. Chem. Phys.* **1957**, *26*, 1354.
(45) Prins, R.; Reinders, F. J. *Chem. Phys. Lett.* **1969**, *3*, 45.
(46) Keulen, E.; Jellinek, F. *J. Organomet. Chem.* **1966**, *5*, 490.
(47) Ryan, M. F.; Richardson, D. E.; Lichtenberger, D. L.; Gruhn, N. E. *Organometallics* **1994**, *13*, 1190.
(48) Li, Y.; Baer, T. *J. Phys. Chem. A* **2002**, *106*, 9820.
(49) Meyer, F.; Khan, F. A.; Armentrout, P. B. *J. Am. Chem. Soc.* **1995**, *117*, 9740.
(50) Moore, D. T.; Oomens, J.; van der Meer, A. F. G.; von Helden, G.; Meijer, G.; Valle, J.; Marshall, A. G.; Eyler, J. R. *ChemPhysChem* **2004**, *5*, 740.
(51) Senko, M. W.; Canterbury, J. D.; Guan, S. H.; Marshall, A. G. *Rapid Commun. Mass Spectrom.* **1996**, *10*, 1839.
(52) Dunbar, R. C. *Mass Spectrom. Rev.* **1992**, *11*, 309.
(53) Kang, H.; Beauchamp, J. L. *J. Phys. Chem.* **1985**, *89*, 3364.
(54) Marshall, A. G.; Wang, T. C. L.; Ricca, T. L. *J. Am. Chem. Soc.* **1985**, *107*, 7893.
(55) Marshall, A. G.; Hendrickson, C. L.; Jackson, G. S. *Mass Spectrom. Rev.* **1998**, *17*, 1.

summed to determine the total fragment yield, which was plotted as a function of the wavelength of FELIX to obtain the infrared (IRMPD) spectrum.

Computational

Computations using density functional theory (DFT) were carried out with the Gaussian 98[56] and Gaussian 03[57] quantum chemistry programs. Our previous work on the binding energetics of first-row transition metal ions to π- and n-donor sites of aniline considered the performance of different functionals, and it was concluded that the MPW1PW91 functional provides a more realistic comparison of the relative binding affinities than the B3LYP functional.[36] Various comparison calculations do not show large differences in the vibrational spectra predicted by these two functionals. Accordingly, all of the calculations described here used the MPW1PW91 functional. The calculations give harmonic normal-mode frequencies and vibrational absorption intensities along with ligand binding thermochemical data.

The triple-ζ 6-311+G(d) basis (polarization and diffuse functions) was used for the Cr center, and the double-ζ 6-31+G(d,p) basis (polarization for all atoms, diffuse functions for all but H) was used for the rest of the atoms. With the exception of the NH_2 inversion mode of aniline, discussed below, various trials with expanded and augmented basis sets did not give important shifts of the predicted IR peak positions, and the basis described was considered to be adequate.

The (0 K) ligand binding energies of the complexes of interest here were calculated at the same level as described above for the vibrational calculations, and the binding energies were corrected for zero-point vibrational energy effects. A uniform correction of 3 kJ mol^{-1} per ligand was subtracted from all of the binding energies as an approximate correction for basis set superposition error (BSSE). Previous work has shown counterpoise BSSE corrections consistently near this value for single-ligand transition metal complexes at this level of calculation,[23] and this generic correction seems to be more than sufficient for the present purposes.

The binding energy of the sextet states is reliably calculated simply by comparing the energies of the complex and the separated reactants. However, the low-spin quartet and doublet states are more complicated since DFT is known to frequently give significant errors in comparing transition metal ion energies in different spin manifolds.[58,59] Two procedures can be used to compensate for this. The direct comparison approach makes a direct comparison of the doublet or quartet complex with the separated reactants, including the sextet ground-state chromium ion. The spin-conserving approach[59] compares the energy of the quartet or doublet complex with the DFT energy for the separated reactants, including the metal ion in the lowest electronic state of the same spin (i.e., quartet or doublet, respectively); following this, the spin-conserving binding energy is corrected by the experimental excitation energy of the chromium atomic ion from its ground state to the relevant excited low-spin state. The excitation energies for the atomic ion are 246 kJ mol^{-1} to the ^{4}G state [3d^5], and 361 kJ mol^{-1} to the ^{2}I state [3d^5]. Note that for free Cr^+, the ^{4}D state [3d^{4}4s^1] is slightly lower in energy; however, it is not considered here because of the unfavorable interaction of the diffuse 4s orbital with the ligand electrons, which shifts the ^{4}D state to higher energy than the ^{4}G once the ligand field becomes appreciable. Bauschlicher[60] and Klippenstein[58] have favored the spin-conserving approach in such situations, but it is not clear which approach should give more accurate binding energy predictions for low-spin complexes, and the associated energy discrepancies should basically be considered as part of the computational uncertainty. All binding energies reported in this work were computed using the direct approach; however, we also indicate those cases where the spin-conserving approach produced significantly different results.

It was not a goal of this work to calculate the most accurate possible binding energies, but rather to use the binding energy calculations to make a preliminary assessment of the most likely binding sites for the two-site ligands and spin states of the complexes. Accordingly, the computations were not carried beyond this reasonably modest basis set, and individual BSSE calculations were not made for each system. Such refinements could be expected to change the comparisons of relative binding energies of the competing binding sites by amounts on the order of 5 kJ mol^{-1}. This would be rather pointless, given that the realistic confidence level of such comparisons with current DFT methods is probably 10−20 kJ mol^{-1}.

An important aspect of the comparisons of the observed and computed IR spectra is the scaling factor to be applied to the computed harmonic vibrational frequencies. For DFT calculations, scaling factors in the range of 0.95−0.98 have been recommended in various studies (for instance, refs 61−64). For the present purposes, the scale factors for these four ligands were calibrated by comparing calculations on the neutral ligands (at the same level of theory as for the complexes) with the experimental IR absorption spectra. The scaling factors determined for the four ligands are not very different, and a uniform scaling factor of 0.960 for the entire set would not give results greatly worse than the individually optimized factors that were used in this study. Details of these comparisons and the scaling factors derived from them are described in the Supporting Information.

Table 1. Thermochemistry of Cr^+ Complexes (DFT calculations)[a]

	Acetophenone			Anisole			Aniline			DMA[c]
ligand	L1	L2	total	L1	L2	total	L1	L2	total	L1
π	143			173			188			202
n	204			151			178			184
$\pi-\pi$		138[b]	282[b]		129[b]	302[b]		146[b]	334[b]	
$\pi-$n $Cr^+(\pi)$-n		170	313		105	278		140	327	
$\pi-$n Cr^+(n)-π		109			127			149		
n−n		180	385		122	273		156	335	

[a] First (L1), second (L2), and overall ligand binding energies (kJ mol^{-1}) are given as ΔH°_{0K} of dissociation. Results are for high-spin (sextet) complexes except as noted; π denotes ring binding of the ligand; n denotes side-chain binding. [b] Low-spin (doublet) complex. [c] *N*,*N*-Dimethyl aniline.

Results

A. Thermochemical Predictions. In our previous communication on the mono- and bis-complexes of aniline with Cr^+, it was shown that the binding site of the chromium ion could not be established on the basis of computational results alone, and thus the experimental spectra were of critical importance.[36] Here, we continue in the same vein, first presenting the calculated thermochemical predictions of binding sites, and for some systems, electronic states as well, and then comparing them with the experimental spectra.

Table 1 shows the computed thermochemistry for all of the mono- and bis-complexes studied here. The "L1" columns give the energy of attaching one ligand to either of the two sites (reaction 1). The "L2" columns give the energy of attaching a second ligand to either of the mono-complex structures to give the two possible resulting bis-complex structures (reaction 2).

(56) Frisch, M. J. et al. *GAUSSIAN 98*; revision A.7; Gaussian Inc.: Pittsburgh, PA, 1998.
(57) Frisch, M. J. et al. *GAUSSIAN 03*; revision B3; Gaussian Inc.: Pittsburgh, PA, 2003.
(58) Yang, C. N.; Klippenstein, S. J. *J. Phys. Chem. A* **1999**, *103*, 1094.
(59) Klippenstein, S. J.; Yang, C. N. *Int. J. Mass. Spectrom.* **2000**, *201*, 253.
(60) Bauschlicher, C. W.; Partridge, H.; Langhoff, S. R. *J. Phys. Chem.* **1992**, *96*, 3273.
(61) Fielicke, A.; Mitric, R.; Meijer, G.; Bonacic-Koutecky, V.; von Helden, G. *J. Am. Chem. Soc.* **2003**, *125*, 15717.
(62) Langhoff, S. R. *J. Phys. Chem.* **1996**, *100*, 2819.
(63) Foresman, J. B.; Frisch, A. E. *Exploring Chemistry with Electronic Structure Methods*, 2nd ed.; Gaussian: Pittsburgh, PA, 1996.
(64) Banisaukas, J.; Szczepanski, J.; Eyler, J. R.; Vala, M.; Hirata, S.; Head-Gordon, M.; Oomens, J.; Meijer, G.; von Helden, G. *J. Phys. Chem. A* **2003**, *107*, 782.

The "total" columns give the overall stability of each of the bis-complexes, that is, the energy to disassemble the bis-complex according to reaction 5.

The thermochemistry for acetophenone is the simplest to interpret since a clear preference for binding at the carbonyl O-atom is demonstrated in all cases. In the mono-complex, O-binding is favored by ~60 kJ mol^{-1}, and for the bis-complex, the O−O structure is also clearly favored in terms of overall stability (energy of disassembly by reaction 5). Moreover, the attachment of the second ligand is strongly favored at the oxygen site, regardless of the mono-complex structure to which it attaches. In fact, the two less-stable geometries for the bis-complex, the ring−ring and ring−O geometries, were not found to be local minima on the potential energy surface. Rather, the data in Table 1 for these two complexes are derived from stationary points found during the optimization that had imaginary frequencies leading to the most stable O−O structure. Thus, it is quite clear from the computational thermochemistry that acetophenone is expected to be exclusively a side-chain binding ligand with Cr^+.

For the anisole and aniline ligands, the situation is somewhat less clear since the energetic difference between binding sites is much smaller, and there is also some ambiguity about the preferred electronic states of the bis-complexes (see below). Anisole seems to prefer binding at the ring-site by 22 kJ mol^{-1} when forming either mono- or bis-complexes, and the overall stability of the $\pi-\pi$ isomer is 30 kJ mol^{-1} greater than that for the n−n isomer. These differences are sufficiently large that one would expect to see only ring-bound complexes of anisole; however, the possibility of a mixture cannot completely be ruled out due to the computational uncertainty. The predictions for aniline are less clear-cut since the energetic differences are even smaller, and so the possibilities of observing isomeric mixtures are greater. This is particularly true for the bis-complex, where the 1 kJ mol^{-1} preference for n−n over $\pi-\pi$ is well within the computational error limits.

The assessment of the preferred binding sites for the bis-complexes of these two ligands is intimately tied to the question of the electronic state of the chromium. Depending on the strength of the ligand field, the interaction of the chromium d-electrons with the filled and empty orbitals of the aromatic π-systems can lead to the stabilization of a low-spin excited state (quartet or doublet) in contrast to the high-spin sextet ground state of free Cr^+ (see Discussion section for a more detailed description). In our previous work on the Cr^+−aniline complexes, we assumed a sextet state for both the mono- and bis-complexes, but that assumption definitely needs to be re-evaluated. As mentioned in the Introduction, such a promotion to a low-spin state is in fact expected for Cr^+ in bis-aromatic π-complexes; thus, it is important to consider different electronic states for these systems.

Table 2 summarizes the important thermochemistry for the different electronic states of chromium with the ligands studied here. Clearly, the ring-bound mono-complexes are expected to be high-spin sextet complexes for all ligands. This is also the case for the preferred n−n bis-complex of acetophenone. In contrast, the differences between the sextet and doublet states of the ring-bound bis-complexes of aniline and anisole are well within the error margins of the calculations, and so no preference can be determined. In fact, the small (1−3 kJ mol^{-1}) indicated preference for low-spin actually reverses when the spin-conserving approach (see Computational section) is used. Thus, as with the binding geometries, the aniline and anisole ligands produce complexes where the electronic state of the chromium also cannot be reliably determined by computation alone.

Table 2. Electronic Spin State Thermochemistry[a]

	Acetophenone			Anisole			Aniline		
ligand	sext.	quart.	doub.	sext.	quart.	doub.	sext.	quart.	doub.
π	143		−57[b]	173	62	−62[b]	188	67	15
$\pi-\pi$	251		282	299	265	302	334	302	334
n−n	385	239		273			335		

[a] The enthalpy (ΔH°_{0K}) for disassembly of the complex according to reaction 3 or 5 (kJ mol^{-1}); π denotes ring binding of the ligand; n denotes side-chain binding. [b] Negative values in the table indicate that the corresponding low-spin complex can spontaneously dissociate into free ligand plus Cr^+ in its ^6S state.

B. Spectroscopic Results. The IRMPD spectra of the four ligand systems are presented below in comparison with DFT-computed spectra of the likely structures and electronic states. Comparisons with experimental spectra of the neutral ligands[65] are also presented, along with comparisons between mono- and bis-complexes of the same ligand (where both spectra are available). As an aid to viewing the numerous curves, note that IRMPD spectra of mono- and bis-complexes are displayed in green and blue, respectively, neutral ligand spectra are in black, and DFT calculations are in red. For the aniline, anisole, and acetophenone systems, the calculated stick spectra were convoluted with a 15 cm^{-1} broad (fwhm) Gaussian line shape, while for dimethyl aniline, where the experimental spectra appear to involve much greater line broadening, a 30 cm^{-1} Gaussian shape was used.

1. Acetophenone. The IRMPD spectrum of the bis-complex is displayed in Figure 1 in comparison with the computed spectra of the three isomeric structures, and also in comparison with the spectrum of the neutral ligand.[65] The experimental spectrum actually consists of two overlapping traces taken with different laser powers. The intense bands above 1200 cm^{-1} were unresolved at full laser power, presumably due to power broadening, and 5 dB of attenuation (factor of 3 reduction in laser power) was required to obtain the resolution shown in the plot. On the other hand, the weaker bands below 1200 cm^{-1} were not observed at the lower power setting, and thus required a 0 dB (full power) scan.

There are two notable diagnostic features showing that the experimental spectrum corresponds to the O−O bound structure. One is the C═O stretching mode, which is at about 1770 cm^{-1} for the ring-bound ligand, and is shifted (and split) to a group of peaks near 1600 cm^{-1} for the O-bound ligand. The only band observed experimentally in this region is centered at 1600 cm^{-1}, and there is no trace of a free-CO stretch to the blue of this band. The other diagnostic feature is the mode having largely C−C stretching character (bond between the ring carbon and the carbonyl carbon), which should be at 1250 cm^{-1} for a ring-bound ligand, but at 1300 cm^{-1} for an O-bound ligand. Again, the IRMPD spectrum matches the O-bound prediction of a peak at 1300 cm^{-1}.

(65) NIST Mass Spec Data Center, S. E. Stein, director, "Infrared Spectra" in *NIST Chemistry WebBook, NIST Standard Reference Database Number 69*; Linstrom, P. J., Mallard, W. G., Eds.; National Institute of Standards and Technology, 2003.

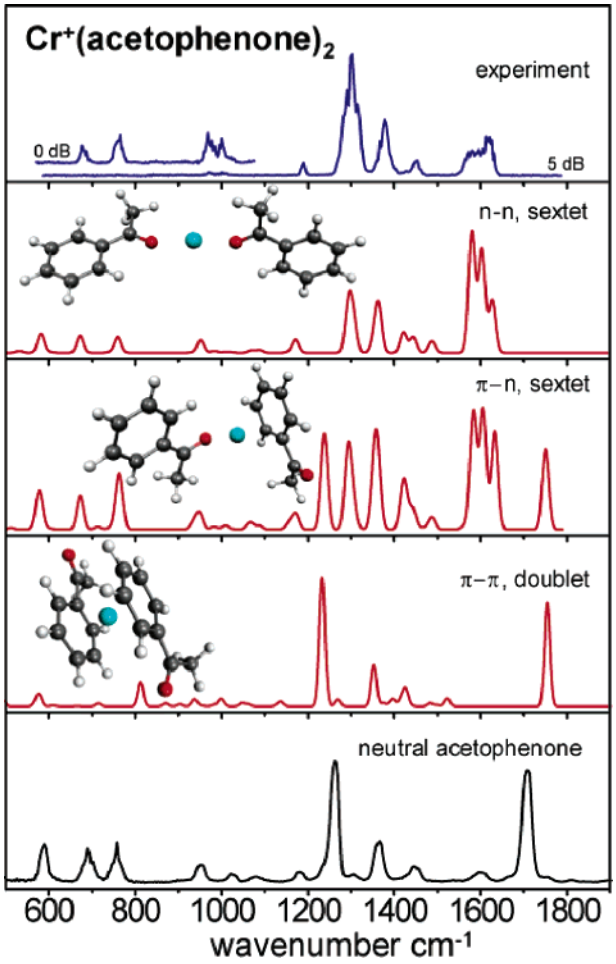

Figure 1. Experimental IRMPD spectrum of Cr^+−acetophenone bis-complex, compared with DFT predictions for different binding sites and electronic states (as indicated). The lower panel shows the FTIR spectrum of neutral acetophenone.[65] The region below 1100 cm^{-1} was re-scanned with 3 times higher laser power to bring out the weaker spectral features.

The DFT-predicted spectra suggest no significant coupling of the two ligands with respect to the normal modes in this frequency range, so that each of the bis-complex structures is predicted to show a spectrum matching a superposition of the spectra of the two corresponding mono-complex spectra. This decoupling breaks down at lower frequencies (below 500 cm^{-1}) for the normal modes corresponding to large-scale motions of the two ligands. However, the modes relevant to the 500−2000 cm^{-1} wavelength region of interest here are all localized within a single ligand. The experimental spectrum is expected to reveal even a minor fraction (a few percent) of the population having a ring-bound ligand, and it is seen that there is no trace of the spectroscopic signature of such a ligand.

The bottom panel of Figure 1 shows the FTIR spectrum of neutral acetophenone for comparison.[65] While there is a qualitative resemblance with the IRMPD spectrum in the figure, it is clear that the bands near 1300 and 1700 cm^{-1} are strongly perturbed in the latter. As mentioned above, these correspond to modes with mostly side-chain character, providing independent corroboration that acetophenone binds to the chromium ion through the carbonyl group. Thus it is clear that acetophenone is a purely oxygen-binding ligand, as predicted by the DFT calculations.

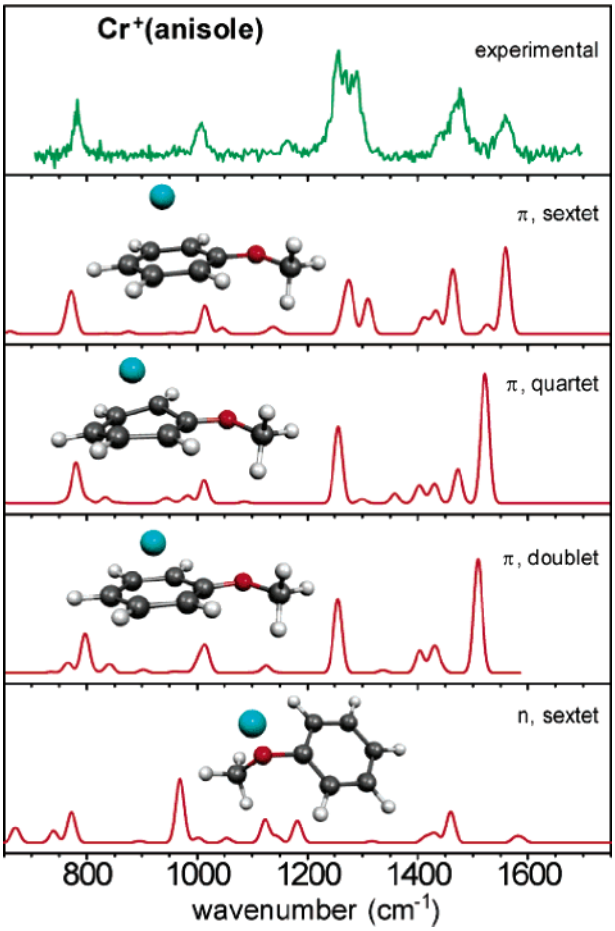

Figure 2. Experimental IRMPD spectrum of Cr^+−anisole mono-complex, compared with DFT predictions for different binding sites and electronic states (as indicated); the relative scales for all calculated spectra are the same.

2. Anisole. Figure 2 shows the IRMPD spectrum of the mono-complex, along with DFT predictions. Agreement with the predicted ring-bound sextet spectrum is excellent, with the most definitive structurally diagnostic features arising from C−O stretching motions. The O−phenyl stretches are predicted to give a pair of strong peaks in the 1300 cm^{-1} vicinity for the ring-bound structure, which are shifted to the 1150 cm^{-1} region for the O-bound structure. The O−methyl stretch gives rise to peaks at 1010 and 980 cm^{-1} in the π- and n-bound structures, respectively, with the latter showing a large increase in intensity. The pair of peaks at 1450 and 1550 cm^{-1} in the ring-bound spectrum match very well with the experimental spectrum and are primarily ring deformation modes (CC stretching and CH in-plane bending character), although there is a small amount of O−phenyl stretching mixed in as well. The corresponding peaks are significantly reduced in intensity in the O-bound spectrum. Considering their highly unfavorable thermochemistries relative to the sextet state (Table 2), the lower-spin ring-bound quartet and doublet states of the mono-complex are not expected to be observed, as is strongly confirmed by the spectra. For example, both spectra from lower spin states differ significantly from the sextet state in the predicted positions of the diagnostic features in the 1400−1600 cm^{-1} region.

Figure 3 shows the DFT-predicted spectra for the bis-complex along with the IRMPD spectrum. It can immediately be seen that, as with the mono-complex, the possibility of O-bound

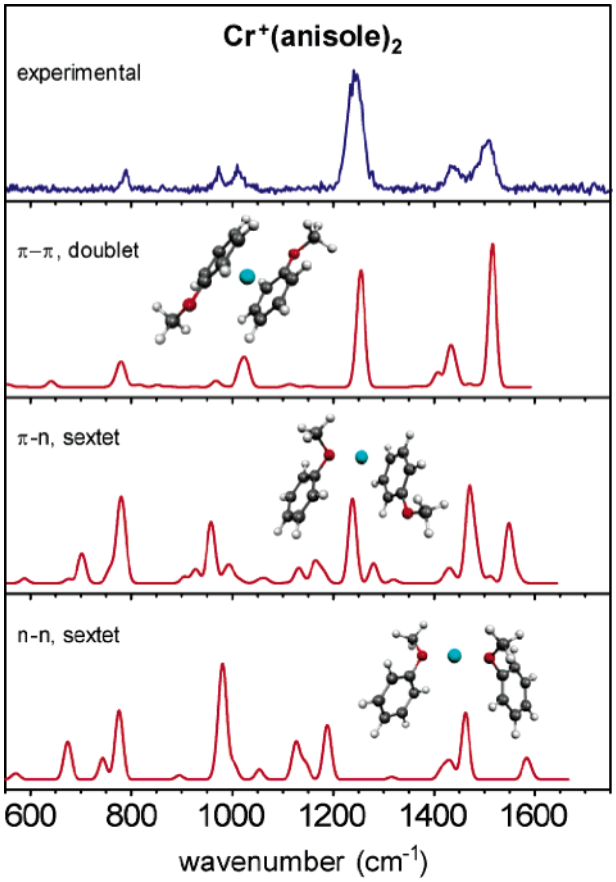

Figure 3. Experimental IRMPD spectrum of Cr^+−anisole bis-complex, compared with DFT predictions for different binding sites (as indicated).

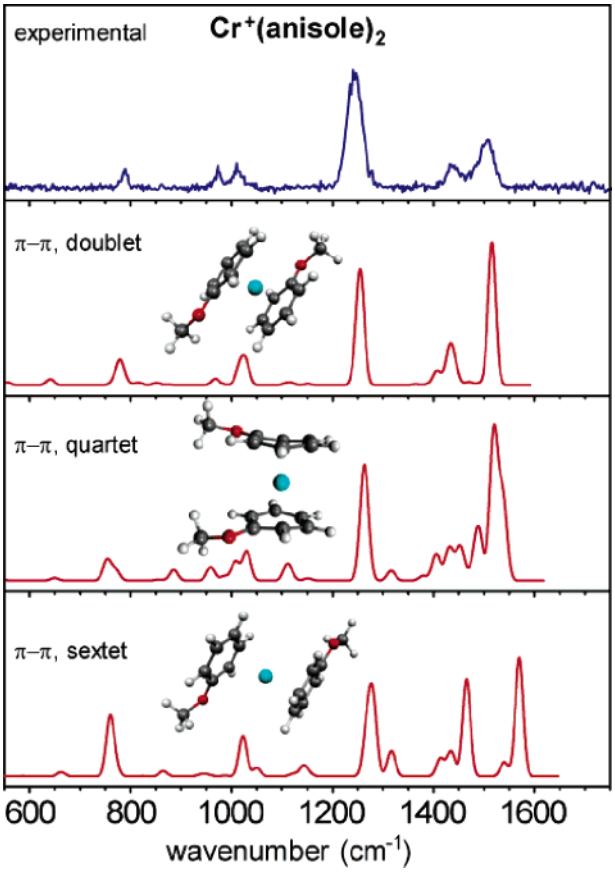

Figure 4. Experimental IRMPD spectrum of Cr^+−anisole bis-complex, compared with DFT predictions for $\pi-\pi$ structures in different electronic states (as indicated).

ligands seems very unlikely. The diagnostic features expected for O-bound ligands are a peak at 700 cm^{-1}, a strong peak near 960 cm^{-1}, and a pair of peaks in the 1100−1200 cm^{-1} region. These predicted features are not matched by the experimental spectrum, and in general, the agreement with the predicted spectra for the exclusively ring-bound geometry is much better.

Figure 4 shows DFT-calculated spectra for the different electronic states of the ring−ring-bound complex in comparison with those of the IRMPD spectrum. The calculated doublet spectrum shows the best correspondence with the experiment, in that the positions of all the strong features in the experimental spectrum are most closely reproduced. The sextet state can be ruled out based on the comparison of the spectrum with the calculation since the fit to the major peaks is generally quite poor for this spin state. Even if an independent scaling factor were used for the sextet spectrum, the doublet assignment would be heavily favored because the relative peak spacings match up much better with the experimental spectrum. The quartet state is a more reasonable possibility, and in this case, the agreement of the calculation is sufficiently close so that a component of this spin state in the ion population cannot be ruled out on spectroscopic grounds alone. The feature of the quartet DFT calculation that corresponds least well to the IRMPD spectrum is the predicted congestion in the 1400−1500 cm^{-1} region, but this is arguably only a minor discrepancy. However, in light of the long relaxation time (3 s) allowed in the experiment and the much lower binding energy predicted by the DFT calculations (quartet is >40 kJ mol^{-1} higher, Table 2), it seems unlikely that any unrelaxed quartet complexes were present when the data were recorded. Thus, the assignment of this structure as a low-spin (probably doublet state) complex with two ring-bound ligands seems very firm.

The bis-complexes can adopt a number of conformations based on the nearly free rotation of the two ligands relative to each other. As an indication of whether this conformational freedom has any importance to the present work, calculations were made of two ring−ring-bound conformers, one (eclipsed) with the side-chains adjacent, and the other (opposed) with them on opposite sides. The energies of the two structures are essentially equal (within 1 or 2 kJ mol^{-1}). Moreover, they are predicted to have nearly indistinguishable IR spectra (as shown in Figure S3 of the Supporting Information). On the basis of these results, the choice of the conformer used for the calculation and the comparison with the experiment was considered to be unimportant.

3. Aniline. Figures 5 and 6 reproduce the IRMPD spectra of the mono- and bis-complexes, respectively, which were previously reported in ref 36, along with the new DFT predictions. As in the earlier work, comparison with the calculations strongly suggests that aniline is only present in the complexes as a ring-bound ligand. The structurally diagnostic features are the peak near 1300 cm^{-1} predicted for the ring-bound ligand, and the peak at 1050−1100 cm^{-1} predicted for the N-bound ligand. The latter would correspond to the frustrated inversion mode of the NH_2 group when bound to the Cr^+ and, thus, be indicative of binding to the nitrogen. Thus it seems that, although the computed thermochemistry suggests binding to the N-atom

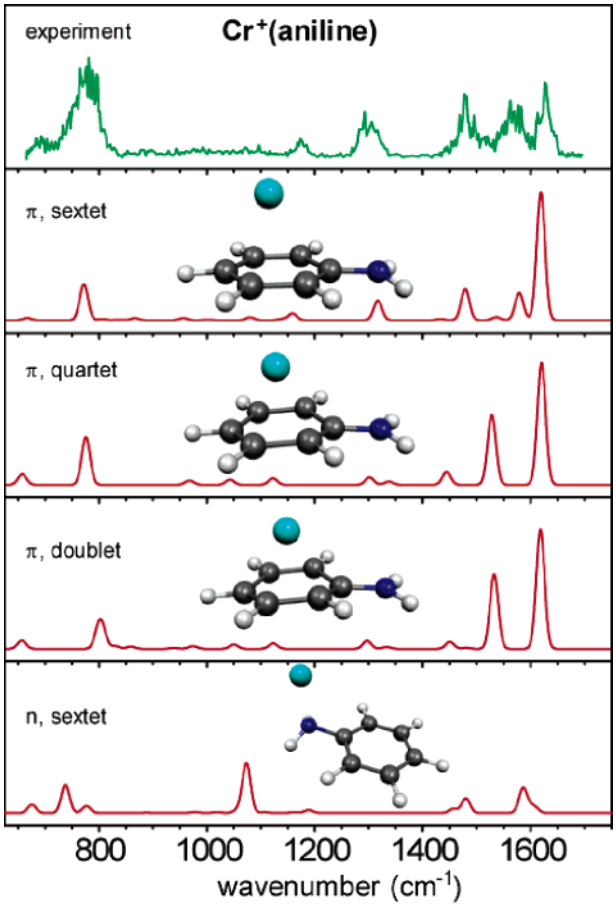

Figure 5. Experimental IRMPD spectrum of Cr^+−aniline mono-complex, compared with DFT predictions for different binding sites and electronic states (as indicated); relative scales for all calculated spectra are the same.

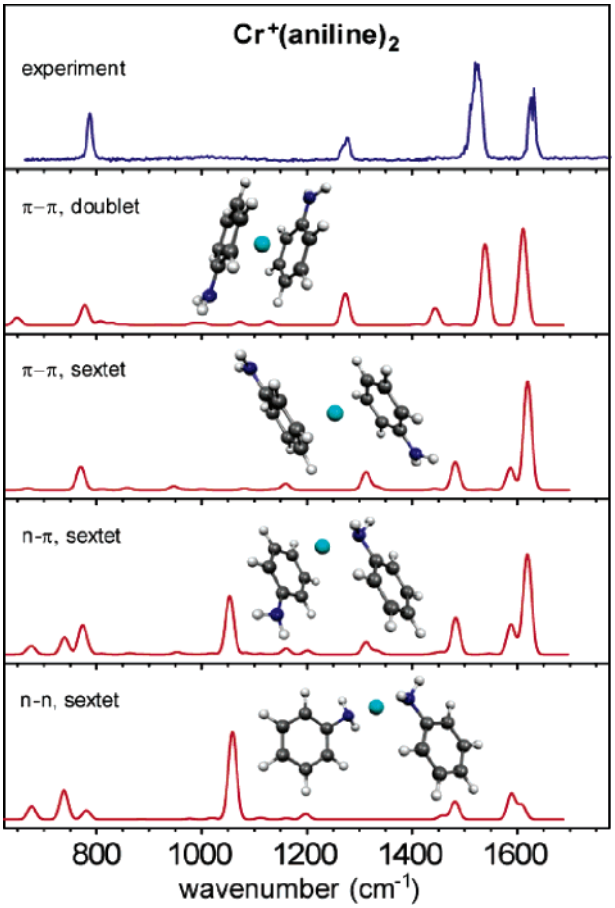

Figure 6. Experimental IRMPD spectrum of Cr^+−aniline bis-complex, compared with DFT predictions for different binding sites and electronic states (as indicated).

might be expected as well, aniline, like anisole, is exclusively a ring-binding ligand with Cr^+.

With respect to the question of the spin states in the ring-bound complexes, the situation is similar to that discussed above for anisole. The 1450−1650 cm^{-1} region is highly diagnostic for high-spin versus low-spin character, and the agreement with the experimental spectrum in this region, along with other less dramatic differences in the predicted spectra, indicates that the mono-complex is high-spin (sextet) and the bis-complex is low-spin (doublet). Certainly the sextet $\pi-\pi$ complex, which had essentially the same predicted thermochemistry as that of the doublet $\pi-\pi$ (Table 1), can be ruled out on the basis of the comparison with the IRMPD spectrum. As observed for anisole, the quartet state spectrum predicted for the $\pi-\pi$ aniline bis-complex gives an only slightly worse match to the experiment than that of the doublet state (see Figure S4 in the Supporting Information). However, as with anisole, the unfavorable thermochemistry of the quartet state (Table 2) makes it unlikely that this state comprises a significant part of the population reflected in the IRMPD spectrum, considering the long relaxation delay allowed in the experiment.

One point that is slightly puzzling is the absence of any experimental feature corresponding to the peak near 1450 cm^{-1} in the calculated spectrum of the doublet bis-complex. Vibrational mode analysis shows that the "missing" peak corresponds to a ring-deformation mode. The dependence of this feature on the different rotational conformations of the aniline ligands was checked, but as with anisole, there was virtually no difference between the calculated spectra for the different rotamers. One potential explanation is that the predicted intensity of this feature in the calculation is a bit too high, and that the actual absorption cross-section is not large enough for the IRMPD mechanism to induce any fragmentation. Alternatively, the IRMPD intensity might also be reduced if the anharmonicity of the associated mode were quite high; however, no evidence of such effects for ring deformation modes of aromatic systems has been reported to date.

4. Dimethyl Aniline. Only the mono-complex of *N*,*N*-dimethyl aniline (DMA) was studied, and the thermochemistry (Table 1) indicates that it favors ring binding. The computational preference over N binding (19 kJ mol^{-1}) is greater than that for aniline, but not by a large enough margin to be conclusive. The IRMPD spectrum is shown along with the DFT predictions in Figure 7 and also the spectrum of neutral DMA[65] in the bottom panel. It is immediately apparent that, unlike the other ligands studied here, the experimental spectrum of the DMA complex contains many broad, overlapping features and thus does not provide a definitive determination of the binding site when compared with the calculated spectra. Some of the spectral confusion could potentially come from power broadening; however, re-measuring the spectrum at lower laser power did not significantly enhance the resolution.

The only feature that shows a clear correspondence with the calculated spectra is the peak near 775 cm^{-1}, which unfortu-

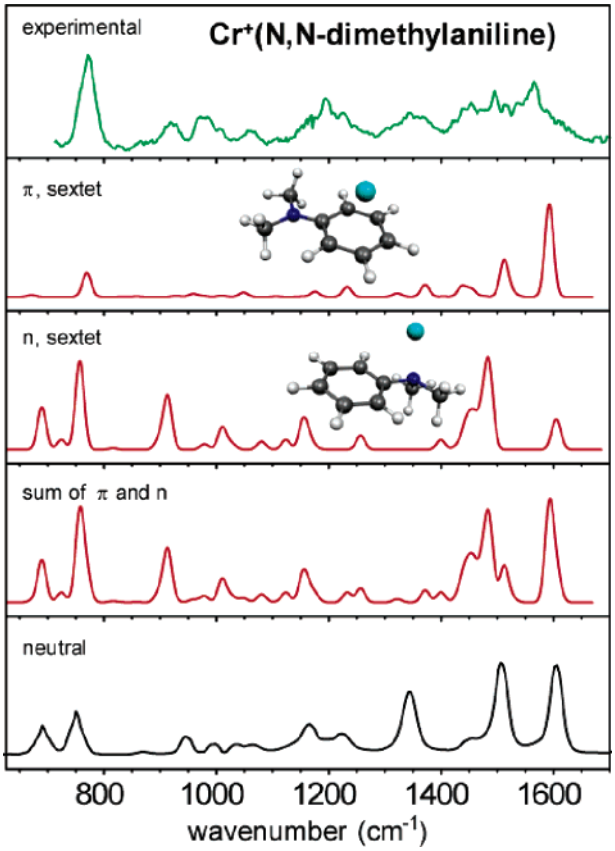

Figure 7. Experimental IRMPD spectrum of Cr^+−*N*,*N*-dimethyl aniline mono-complex, compared with DFT predictions for ring and side-chain binding (as indicated). The summed spectrum was composed using the same relative intensity for the strongest features in the N-bound and ring-bound spectra (see text). The bottom panel shows the spectrum of neutral *N*,*N*-DMA.[65]

nately is not at all diagnostic for a particular binding site. It can be generally observed, however, that the presence of peaks in the 900−1200 cm^{-1} region of the spectrum tends to support the presence of N-bound complexes. Similarly, the rather strong absorption near 1600 cm^{-1} supports the presence of ring-bound structures. Thus it seems quite possible that the experimental spectrum reflects a mixture of the two isomers; as an indication of whether this is a reasonable suggestion, a summed spectrum composed of the DFT predictions for the N-bound and ring-bound structures (assuming the same relative intensity for the strongest features) was constructed, as shown in Figure 7. This summed spectrum yields marginally better agreement with the experiment, and it is conceivable that further improvement could be gained by optimizing the relative contributions of the two structural isomers. However, such treatments would require a good correspondence between the relative intensities of the bands in the calculated and experimental spectra, and this cannot generally be assumed for IRMPD data, especially for congested spectra.[31] In any case, there is not sufficient agreement of the peak positions in any of the calculated spectra to pursue the assignment any further.

Discussion

One of the most intriguing results of this work is that the experimental vibrational spectra can clearly distinguish between different electronic states of the transition metal centers in the complexes. Some evidence of this has been observed previously in the IRMPD spectra of mono- and bis-complexes of benzene with transition metals;[34,37,38] however, the richer vibrational spectra of the functionalized aromatic molecules studied here make the spectral changes more apparent. In addition, the current study demonstrates that the infrared spectra can be used to detect the onset of spin promotion as a function of coordination number and, hence, ligand field strength in gas-phase organometallic complexes. Specifically, it was found that, as expected, the ligand field of two ring-bound aromatic ligands is sufficient to promote the Cr^+ to a doublet configuration, while a single ligand is not, nor is the field from two side-chain bound ligands.

One can build up a first-order understanding of these effects by considering the interactions of the d-orbitals on the metal center with the molecular orbitals at the binding site on the ligand. Such explanations have been discussed extensively in the literature,[7,17] so only a brief review is given here. In the weak field limit, the most significant interaction is the Pauli repulsion between filled (or partially filled) orbitals on the different sites. The chromium monocation has a sextet ground state configuration ($3d^5$, $4s^0$), resulting in a half-filled d-shell, with one electron in each orbital. For an aromatic ligand (taking the *z*-axis as normal to the ring plane), the d_{xz} and d_{yz} orbitals will experience the strongest initial repulsion, causing them to shift to higher energies, while the d_{z^2}, $d_{x^2-y^2}$ and d_{xy} orbitals remain relatively unaffected. As the Cr−ligand distance decreases, the "Pauli pressure" on the d_{xz} and d_{yz} orbitals increases until the destabilization becomes comparable with the energy required to promote the Cr^+ from the sextet to the doublet state (∼360 kJ mol^{-1}), and then, the electrons in these orbitals will be paired into the d_{xy} and $d_{x^2-y^2}$ orbitals. By now, the complex is in the strong ligand field limit, where there is an appreciable overlap of the metal and ligand orbitals. The (now empty) d_{xz} and d_{yz} orbitals can then hybridize with the empty 4s and 4p orbitals to form a set of orbitals to accept electron density from the aromatic ligands, increasing the binding strength.[7] There is also the possibility of back-donation from the Cr d_{xy} and $d_{x^2-y^2}$ orbitals into the π^*-aromatic orbitals of the ligand, although at least in the case of the neutral dibenzene chromium complex, this effect is small.[7]

For side-chain binding, the general effects described above still hold, although in the weak field limit, it is the d_{z^2} orbital that has the most unfavorable interaction with the filled n-orbital of the ligand, while the d_{xz} and d_{yz} orbitals are relatively unaffected. However, the more localized nature of the electron densities at the binding sites means that more ligands are required to reach the strong field limit where spin promotion of the metal center is favorable, and thus the complexes remain high-spin for the low coordination numbers ($\leq$2) considered here.

As one would expect based on the discussion above, the interactions of the sextet and doublet states of the chromium ion with the ring-bound ligands are fundamentally different. This can be further appreciated from the drastic difference in the computed Cr−ring distances between the mono- and bis-complexes of both aniline and anisole (Table 3). In fact, this distance is so short in the doublet bis-complexes that the ring−ring distance is comparable to the spacing of the molecular planes in graphite (3.36 Å[66]), indicating that the aromatic

(66) Reynolds, W. N. *The Physical Properties of Graphite*; Elsevier: Oxford, 1968.

Table 3. Structural Parameters (DFT) for Ring-Bound Ligands as a Function of Complexation Number and Electronic State

	Aniline				Anisole			
	r_{CC} (Å)[a]	r_{CN} (Å)	ϕ (°)[b]	r_{Cr} (Å)[c]	r_{CC} (Å)[a]	r_{OPh} (Å)	r_{OMe} (Å)	r_{Cr} (Å)[c]
free ligand	1.396	1.391	38.7		1.395	1.359	1.409	
mono-complex (sextet)	1.410	1.356	18.1	2.084	1.409	1.330	1.428	2.092
bis-complex (doublet)	1.418	1.372	31.6	1.662	1.417	1.340	1.424	1.651

[a] Average value of CC bond lengths in aromatic ring. [b] Angle between planes of phenyl and NH_2 groups. [c] Cr−ring distance.

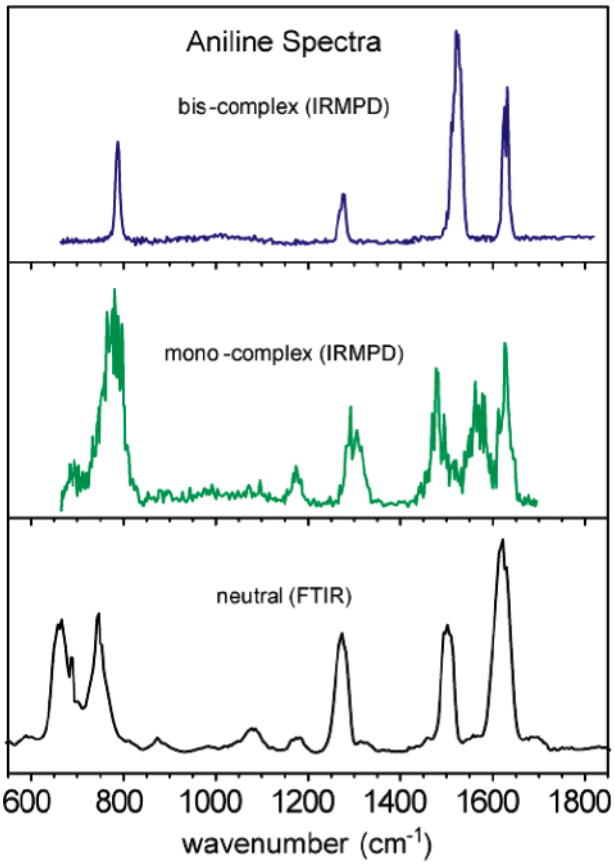

Figure 8. IRMPD spectra of mono- and bis-complexes of aniline with Cr^+, compared with the spectrum of neutral aniline.[65]

π-clouds are in contact, with the Cr^+ intercalated between them (see Figure S5 in the Supporting Information). It is important to realize it is the electronic state of the Cr^+, as opposed to the coordination number, which determines the Cr−ring bond length. The doublet mono-complexes also have Cr−ring distances of ∼1.6 Å, while the sextet bis-complexes have values in the range of 2.0−2.2 Å (see Supporting Information). The effects of this can be seen in the calculated spectra. For example, the mono- and bis-complexes of ring-bound aniline in the sextet state (see Figures 5 and 6) are clearly much more similar than those for different electronic states with the same coordination number, particularly in the region between 1400 and 1650 cm^{-1}. It is therefore worthwhile to compare the spectra and structural data for the mono- and bis-complexes with the data for the free ligands to identify any significant trends.

Figures 8 and 9 show the experimental IRMPD spectra for the Cr^+ mono- and bis-complexes of aniline and anisole, respectively, along with gas-phase FTIR spectra of the neutral ligands.[65] The observed peaks are collected in Table 4, along

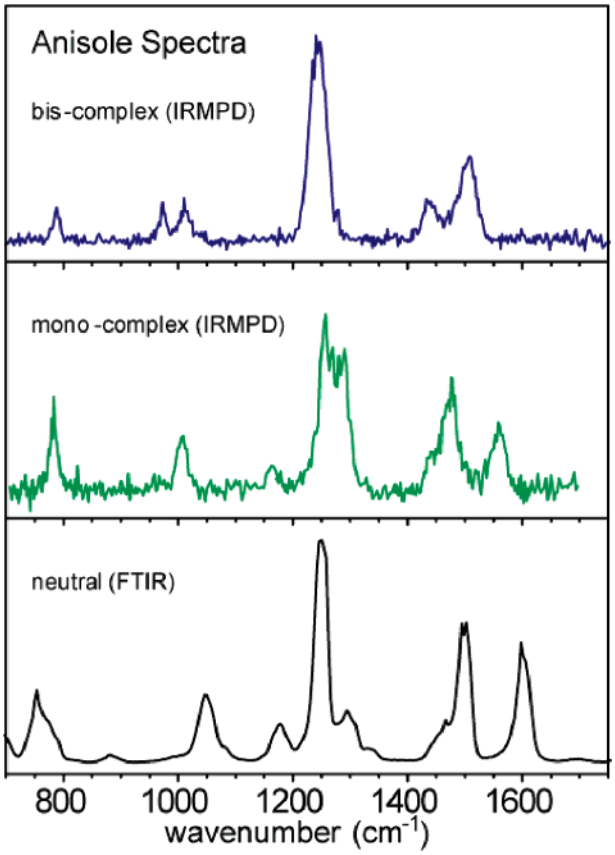

Figure 9. IRMPD spectra of mono- and bis-complexes of anisole with Cr^+, compared with the spectrum of neutral anisole.[65]

Table 4. Experimental Vibrational Frequencies and Assignments for Neutral Anisole and Aniline, as Well as Mono- and Bis-Complexes with Cr^+ (ipb = in-plane bend, opb = out-of-plane bend)

Aniline				Anisole			
FTIR[a]	mono	bis	assignment[b]	FTIR[a]	mono	bis	assignment[b]
667			CH opb	759	783	788	CH opb
746	775	787	CH opb	1049	1006	972	O-Me str. CH ipb
1076			CH ipb			1012	
1176	1174		CH ipb	1178	1165		CH ipb
1272	1300	1275	CN str.	1249	1257	1244	O−Ph str. CH ipb
1502	1481	*1444*[c]	CC str.		1289		
1601[c]	1628	1628	NH_2ipb	1300			CC str.
1620	1567	1522	CC str. CH ipb	1457	1442	1442[d]	CH_3 bend
				1499	1474	1442[d]	CC str. CH ipb
				1601	1558	1505	CC str.

[a] From ref 65. [b] Based on calculated DFT normal modes, taken from sextet and doublet states for mono- and bis-complexes, respectively. [c] Unobserved, low-intensity modes, scaled DFT value only. [d] DFT predicts overlapping bands of equal intensity.

with the assignments based on the calculated normal modes. For the most part, the character of a given vibrational mode is well correlated between the neutral molecule and the complexes, although the frequencies are significantly shifted for certain modes. For example, the modes with primarily CC stretching character are strongly and progressively red shifted as they go from neutral ligand to the mono- to the bis-complex. There is a different trend shown by modes involving the stretching of

the "link" between the ring and side-chain (C−N for aniline, O−phenyl for anisole); these show a blue shift in the mono-complexes, but remain relatively unchanged in the bis-complexes.

These trends are nicely consistent with the calculated structural parameters for aniline and anisole, both as free molecules and in the Cr^+ complexes; these data are collected in Table 3. For both species, the average CC bond length in the aromatic rings shows a steady increase that follows the red-shift trend observed in the experimental spectra. Since an increasing bond length is generally accompanied by a decrease in the associated force constant for stretching motion, this is precisely the effect one might have expected. There is an analogous relationship for the bond lengths connected to the link stretching modes (CN and O−phenyl), which are shortest in the mono-complexes, where the frequencies are highest. In general, this correlation of blue (red) shifts with bond contraction (extension) is observed for all of the stretching modes in the two series. The CH bending modes remain relatively unperturbed except for the out-of-plane modes around 750−800 cm^{-1}, which show a progressive blue shift as the Cr−ring distance decreases from neutral to mono to bis. This trend has been reported previously for ring-bound complexes of metal ions and aromatic molecules and is attributed to the repulsive interaction of the H-atoms with the metal atom on one side of the ring.[30]

Some of the modes also show significant changes in intensity between the free ligands and the complexes. For example, the NH_2 in-plane bending or "scissor" mode of aniline, which is assigned to the strong bands farthest to the blue in the Cr^+ complexes, is rather weak in the neutral molecule. On the other hand, there is an aniline ring mode near 1500 cm^{-1} that is rather pronounced in the spectra of the neutral and mono-complex, but which disappears in the bis-complex spectrum. These differences are perhaps not so surprising, given that the changes induced by the Cr^+ in the electronic distributions of the ligands can also affect the electronic components of the vibrational transition dipoles, which give rise to the infrared intensities.

Ideally, one would like to go further and connect the structural and spectroscopic trends in the data to the changes in the electronic distributions of the ligands due to the interactions with the different electronic states of Cr^+. In some cases, the interpretation is fairly self-evident; the observed trend in the CC stretching vibrations and bond lengths with electronic state follows logically from the observation that the electrophilic Cr^+ will tend to withdraw electron density from the aromatic π-system, and this effect will be greater when the Cr−ring separation is smaller. Other cases are not so clear, however. For example, the angle between the NH_2 and phenyl planes (ϕ) in the doublet bis-complex (32°) is much closer to that of neutral aniline (39°) than for the sextet mono-complex (18°). It is known that the geometry of the NH_2 group in aniline is quite sensitive to the electronic state, becoming planar in the aniline cation[67] and "quasi-planar" in the S_1 excited state of the neutral.[68] In fact, the calculated structure of the S_1 electronic excited state of aniline is quite analogous to that of the Cr^+ mono-complex, having a CN bond length of 1.347 Å and $\phi = 20°$.[68] As an initial attempt to explain this, we calculated the charge on the Cr center by applying natural population analysis (NPA)[69] to the DFT electron densities for the complexes, obtaining values of 0.98 and 0.22 for the mono- and bis-complexes, respectively. The latter result is particularly striking since it suggests that most of the positive charge is localized on the aniline ligands, as opposed to the metal center. However, these results also make it clear that a full understanding of the mechanisms driving these spectral and structural trends will require a detailed computational analysis that is beyond the scope of the present work.

Conclusions

The primary goals of this study were to use the IRMPD spectra to establish the binding site and electronic state of the chromium ion in complexes formed with the various ligands and to compare the results with predictions based on the computational thermochemistry to assess the performance of the DFT methods used. On the first point, we were successful for three of the four ligands studied: acetophenone, anisole, and aniline. All of these complexes exhibited spectral features that were sufficiently diagnostic to allow unambiguous assignment of the binding sites of the Cr^+: ring binding for aniline and anisole and side-chain binding for acetophenone. For the ring-binding ligands (anisole and aniline), the mono-complexes were found to have high-spin sextet states, while the bis-complexes were found to have low-spin (probably doublet) states. These experiments provide an exceptional opportunity for direct observation of spin promotion as a function of coordination number for an organometallic complex in the gas phase. The fourth ligand, *N*,*N*-dimethyl aniline, yielded an experimental spectrum that was quite congested, and neither of the calculated spectra for the side-chain and ring-bound isomers was a close match. Hence, a definitive assignment of the binding site was not possible, although the observed spectrum may well reflect a mixture of comparable amounts of both isomers.

On the question of the computational thermochemical predictions of binding sites and electronic states, the experimental results did not conflict with any of the computed results for the three ligands wherever experimental assignments were possible. The clear predictions of a ring-bound sextet state for anisole mono-complex, a ring−ring-bound complex for the anisole bis-complex, and of an O−O bound sextet for acetophenone bis-complex were in agreement with the observed spectra. However, although the anisole bis-complex was clearly predicted to have ring−ring geometry, the computations could not distinguish between the high- (sextet) and low-spin (doublet and quartet) possibilities, and the assignment to a $\pi-\pi$-bound, low-spin (probably doublet) state complex could ultimately only be made from the observed spectrum. In the case of aniline mono-complex, where the DFT/MPW1PW91 calculation gave a slight preference to the ring-bound sextet, the observed spectrum supported this prediction, with no indication of an admixture of N-bound complexes. For the bis-complex of aniline, the calculations gave no useful prediction between the three possibilities of the ring−ring sextet, the ring−ring low-spin, and the N−N sextet. Accordingly, the identification of the complex as the ring−ring low-spin (probably doublet) was entirely dependent on the observed spectrum.

An ancillary result was the comparison of the IR spectra of the neutral ligands with DFT calculations at this level (see

(67) Song, X. B.; Yang, M.; Davidson, E. R.; Reilly, J. P. *J. Chem. Phys.* **1993**, *99*, 3224.
(68) Sinclair, W. E.; Pratt, D. W. *J. Chem. Phys.* **1996**, *105*, 7942.
(69) Reed, A. E.; Weinstock, R. B.; Weinhold, F. *J. Chem. Phys.* **1985**, *83*, 735.

Supporting Information). The calculations gave almost uniformly good predictions of the spectra after scaling the calculated frequencies by factors ranging from 0.951 to 0.965. For the major peaks in the neutral ligand spectra, deviations between observed and calculated frequencies were of the order of 10−15 cm^{-1}, and not larger than 25 cm^{-1}. This provided a baseline for judging when deviations found in the spectra of the ions could be considered as more than random errors of the computational comparisons. The main exception was the nitrogen inversion peak of aniline, which was not successfully treated by these harmonic vibrational calculations. Relative peak intensities were usually, but not always, estimated within a factor of 2, a rather low degree of predictive accuracy which can be attributed to the nonlinear character of the IRMPD process, as well as to computational inaccuracies.

Acknowledgment. This work is part of the research program of FOM, which is financially supported by the Nederlandse Organisatie voor Wetenschappelijk Onderzoek (NWO). R.C.D. acknowledges the support of the donors of the Petroleum Research Fund, administered by the American Chemical Society. Construction and shipping of the FT-ICR instrument was made possible with funding from the National High Field FT-ICR Facility (NSF Grant CHE-9909502) at the National High Magnetic Field Laboratory in Tallahassee, Florida.

Supporting Information Available: A description is given of the calibration of scaling factors appropriate for complexes of each ligand by comparison of the neutral ligand IR spectrum with the computed DFT spectrum. Figures showing this comparison for each ligand are given. Figures showing additional DFT-predicted spectra for particular complexes as mentioned in the text are also provided (rotamers of $\pi-\pi$ bis-complexes, electronic states of $Cr^+(aniline)_2$ complex). Larger size views of the computed structures of the complexes are also provided. This material is available free of charge via the Internet at http://pubs.acs.org.

JA042431D